


Early Detection of Cascade Flutter in a Model Aircraft Turbine Using a Methodology Combining Complex Networks and Synchronization

Takayoshi Hachijo¹, Hiroshi Gotoda^{1,*}, Toshio Nishizawa^{2,†} and Junichi Kazawa^{2,‡}

¹*Department of Mechanical Engineering, Tokyo University of Science, 6-3-1 Niijuku, Katsushika-ku, Tokyo 125-8585, Japan*

²*Japan Aerospace Exploration Agency, 7-44-1 Jindaiji-Higashimachi, Chofu-shi, Tokyo 182-8522, Japan*

 (Received 20 January 2020; revised 19 May 2020; accepted 19 June 2020; published 30 July 2020)

We report an experimental study on the early detection of cascade flutter in a model aircraft turbine using a methodology that combines complex networks and synchronization. The network topology constructed from the determinism in the cross-recurrence plot allows us to extract the primary hubs during a transition to cascade flutter. The node strength in the network topology and the synchronization parameter are valid for capturing a precursor of cascade flutter.

DOI: [10.1103/PhysRevApplied.14.014093](https://doi.org/10.1103/PhysRevApplied.14.014093)

I. INTRODUCTION

Aeroelastic instability gives rise to self-excited blade vibrations in an aircraft engine. This unstable phenomenon is referred to as flutter and in some instances leads to the destruction of turbine blades. The physical mechanism responsible for limit-cycle oscillations during flutter, which is strongly associated with mistuning and structural damping, has been extensively examined for various model aircraft turbines [1–3]. The onset of cascade flutter has impeded the technological development of advanced jet engines and its early detection is a longstanding problem in present-day aerospace propulsion engineering. The early detection of flutter using nonlinear time-series analysis has recently been conducted by Venkatramani *et al.* [4,5]. They have discussed the applicability of recurrence quantification analysis and the Hurst exponent for the early detection of flutter on NACA0012 in a wind channel, suggesting the possible existence of a multifractal structure during the dynamical state prior to the onset of flutter.

The synchronization of interacting nonlinear oscillators is a ubiquitous phenomenon and its emergence has attracted significant attention in various fields of natural science and engineering over the past few decades [6]. An important analytical approach to deal with the synchronization is the phase reduction of coupled limit-cycle oscillators [7], and this approach has become widespread in the nonlinear-physics community. The order parameter derived from this approach, which is a well-recognized

measure in time-series analysis in terms of synchronization, has been adopted for propulsion systems such as a land-based gas-turbine engine [8] and a rocket engine [9]. Time-series analysis in terms of complex networks is also a rapidly growing research field [10] and the recent advances in the methodology have yielded significant success in the early detection of dynamical transitions in propulsion systems [11,12]. The importance of complex networks has been shown in the field of applied physics [13,14]. Our main aim in this study is to explore the applicability of a methodology combining complex networks and synchronization to detect a precursor of cascade flutter.

The Japan Aerospace Exploration Agency (JAXA) has recently promoted an advanced-fan-jet-research (aFJR) study [15] as a national project, one of the objectives of which is to suppress cascade flutter in a low-pressure turbine. This project aims to achieve significant progress in the development of environmentally adaptable technology for prospective turbofans with a superhigh bypass ratio. The development of sophisticated methodologies for detecting cascade flutter is an important focus of the project. Here, we attempt to develop a pragmatic methodology for integrating complex networks and synchronization to detect a precursor of cascade flutter in a model aircraft turbine, including the characterization of the dynamic behavior of cascade flutter.

We first characterize the dynamical state of cascade flutter from the viewpoint of statistical complexity. The importance of a statistical complexity-based approach in various physical settings [11,16–23] has recently been shown by one of the present authors. The cycle network proposed by Zhang and Small [24] enables us to clarify pseudoperiodic behavior such as deterministic nonperiodic intercycle

*gotoda@rs.tus.ac.jp

†nishizawa.toshio@jaxa.jp

‡kazawa.junichi@jaxa.jp

dynamics and periodic orbits with correlated noise. In addition to the statistical complexity-based approach, we introduce the cycle network in this study to reveal the pseudoperiodic behavior during cascade flutter. We next visualize the network structure constructed from the determinism in a cross-recurrence plot (CRP) and estimate the node strength in the network topology. We finally estimate the synchronization parameter in the network topology by incorporating the concept of collective synchronization.

This paper is organized into three sections. The experimental system and the mathematical framework of the analytical methods are briefly described in Secs. II and III, respectively. We present the results and discussion in Sec. IV and provide a summary in Sec. V.

II. EXPERIMENTS

Similar to a previous study [25], we employ a low-pressure turbine test rig to represent an important case of cascade flutter in a turbofan-jet-engine system. As shown in Fig. 1, the low-pressure turbine comprises 80 stator vanes. We set the blade aspect ratio to 8.8 to reduce the structural natural frequency and label the blades from 1 to 80 in the clockwise direction. We carry out all the experiments utilizing the altitude test facility of JAXA (JAXA ATF) [26]. The details of the experimental conditions are described in Ref. [25]. In this study, the mass flow rate of inlet air normalized by the designed mass flow rate, denoted as Q , is transiently varied from 59 to 89% as a function of time to trigger cascade flutter. The strain fluctuations ϵ' in the radial direction are measured in a single direction using a strain gauge placed on the pressure side of each turbine blade, near the tip shroud. The sampling frequency of ϵ' is set to 20 kHz.

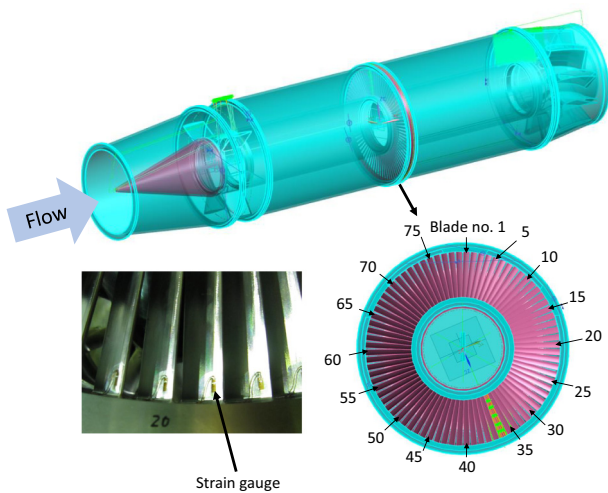


FIG. 1. Low-pressure turbine test rig.

III. MATHEMATICAL FRAMEWORK OF ANALYTICAL METHODS

The cycle-network approach is valid for revealing the dynamical state of strongly periodic-like time series [24]. To construct the cycle network, ϵ' is divided at each local minimum into n cycles $\{C_1, C_2, \dots, C_n\}$. Each cycle C_i corresponds to nodes in the network. The links between nodes are determined by the correlation between the cycles ρ_{ij} [27], defined as follows:

$$\rho_{ij} = \max_{l=0,1,\dots,l_j-l_i} \frac{\text{Cov}[C_i(1:l_i), C_j(1+l:l_i+l)]}{\sqrt{V[C_i(1:l_i)]}\sqrt{V[C_j(1+l:l_i+l)]}}. \quad (1)$$

Here, $C_i(a:b)$ denotes the segment between the a th and b th elements in C_i , $V(\cdot)$ is the variance, and l_i and l_j are the lengths of C_i and C_j , respectively. The number of network nodes n is 1255 for ϵ' during 1 s. The threshold of ρ_{ij} for the transformation into a binary network, which is just above the critical value required to break the network's single giant component in which the subnetworks cross-link spontaneously to form a single giant component [24], is set to 0.99 in this study.

A CRP [28,29] allows us to extract nonlinear interrelations from bivariate time series. The basic idea of the CRP comes from the comparison of the trajectories of two states in the same phase space. The appearance of long diagonal structures in the CRP means the formation of similar forms of dynamic behavior in both time series. The *determinism* in the CRP, which is defined as the ratio of the number of cross-recurrence points forming long diagonal structures to the total number of points, has been proposed as a means of recurrence quantification analysis [30] and is useful for evaluating the similarity of dynamical states between two different systems. One of the present authors [31] has recently adopted the CRP for the analysis of synchronization between two buoyancy-driven turbulent fires. A more recent study on the synchronization of local heat-release-rate fluctuations during thermoacoustic combustion oscillations [32] has shown that the determinism in the CRP can be treated as the connecting strength in weighted networks. On this basis, in this study, we consider the determinism D_{mn} as the connecting strength in the weighted networks between the blades. In other words, D_{mn} corresponds to the mn components in the adjacency matrix in the weighted networks. For the construction of the CRP, the temporal evolutions of ϵ'_m on blade m and ϵ'_n on blade n are simultaneously embedded into the same D -dimensional phase space as $\epsilon_m = [\epsilon'_m(t), \epsilon'_m(t+\tau), \dots, \epsilon'_m(t+(D-1)\tau)]$ and $\epsilon_n = [\epsilon'_n(t), \epsilon'_n(t+\tau), \dots, \epsilon'_n(t+(D-1)\tau)]$, where τ is the embedding delay time. The CRP consists of the matrix component $C_{ij} = \Theta[r - \|\epsilon_m(t_i) - \epsilon_n(t_j)\|]$, where Θ is the Heaviside function, r is the threshold, $\|\cdot\|$ is the

Euclidean norm, and i and j are the arbitrary points in the trajectories in the phase space. D_{mn} is a function of the time distance τ' from the main diagonal line ($i = j$) in the CRP and is computed separately for each diagonal line parallel to the main diagonal line as

$$D_{mn} = \frac{\sum_{l=l_{\min}}^{N_p-\tau'} lp_{\tau'}(l)}{\sum_{l=1}^{N_p-\tau'} lp_{\tau'}(l)}. \quad (2)$$

Here, N_p is the number of phase-space vectors, $p_{\tau'}(l)$ is the frequency distribution of the length l of each diagonal line parallel to the main diagonal line, and l_{\min} is the shortest allowable diagonal line length. l_{\min} is generally set to 2, as the minimum diagonal line length. However, D_{mn} at $l_{\min} = 2$ takes a high value for blades with an extremely low correlation between two strain fluctuations. To solve this problem, we set l_{\min} to 3 in this study. The value of r is determined so as to ensure that the recurrence rate $[= (\sum_{i,j=1}^{N_p} C_{ij})/N_p^2]$ [30] is 0.05. In this study, we set τ' to zero corresponding to the main diagonal line on the CRP, to focus on the degree of the recurrence at the same time. After constructing the weighted networks using D_{mn} at $\tau' = 0$, the node strength I is estimated as

$$I = \sum_n D_{mn}. \quad (3)$$

The dynamics of oscillators coupled through synchronization can be expressed as networks by replacing the oscillators with nodes. The synchronization parameter r_s [33,34], which considers the phase equation describing the dynamics of coupled oscillators, is a useful measure with which to quantify the synchronized state in networks. To estimate r_s , we compute the time average of the order parameter r_{mn} between the m th oscillator and n th oscillator as

$$r_{mn} = \lim_{\Delta t \rightarrow \infty} \frac{1}{\Delta t} \left| \int_t^{t+\Delta t} \exp i[\theta_m(t') - \theta_n(t')] dt' \right|, \quad (4)$$

where Δt is the time interval. $\theta_m(t')$ and $\theta_n(t')$ are the instantaneous phases of $\epsilon'_m(t)$ and $\epsilon'_n(t)$, respectively, obtained by the Hilbert transformation [35]. We estimate r_s corresponding to the average value of nodes in weighted networks:

$$r_s = \frac{1}{\sum_m \sum_n D_{mn}} \sum_m \sum_n D_{mn} r_{mn}, \quad (5)$$

where $0 \leq r_s \leq 1$. $r_s = 1$ corresponds to a completely synchronized state. Note that the number of nodes in weighted networks is set to 80, which is the same as the number of blades in the test rig.

IV. RESULTS AND DISCUSSION

Figure 2 shows the temporal evolution of the strain fluctuations ϵ' at the 50th blade and the corresponding power-spectral density (PSD) with increasing mass flow rate of inlet air Q . Note that the frequency of ϵ' is normalized by that of the first torsional mode during cascade flutter, and the normalized frequency is denoted as f . The amplitude of ϵ' markedly increases at $t \approx 15.0$ s and the distinct peak at $f = 1$ becomes predominant in the power spectra owing to the onset of aeroelastic instability. Here, we examine the dynamical state of ϵ' during cascade flutter using the multiscale complexity-entropy causality plane (CECP) [36] as a statistical complexity-based approach. The multiscale CECP, consisting of the permutation entropy and the Jensen–Shannon statistical complexity, incorporates the variation in the embedding time delay of the phase space. The dynamical state is judged from the shape of the trajectory on the CECP resulting from the change in the embedding time delay (for details of the methodology on the CECP, see Ref. [29]). Figure 3 shows the variations in the permutation entropy H_p and the Jensen–Shannon statistical complexity C_{JS} as a function of the embedding delay time τ , together with the H_p – C_{JS} plane. Extreme values of H_p and C_{JS} simultaneously appear at an interval of 0.8 ms. This interval corresponds to the period of the first torsional mode. We observe the reverse motion of the trajectory of (H_p, C_{JS}) with increasing τ . The important point to note here is that the configuration of the trajectory nearly corresponds to that of noisy periodic limit-cycle oscillations

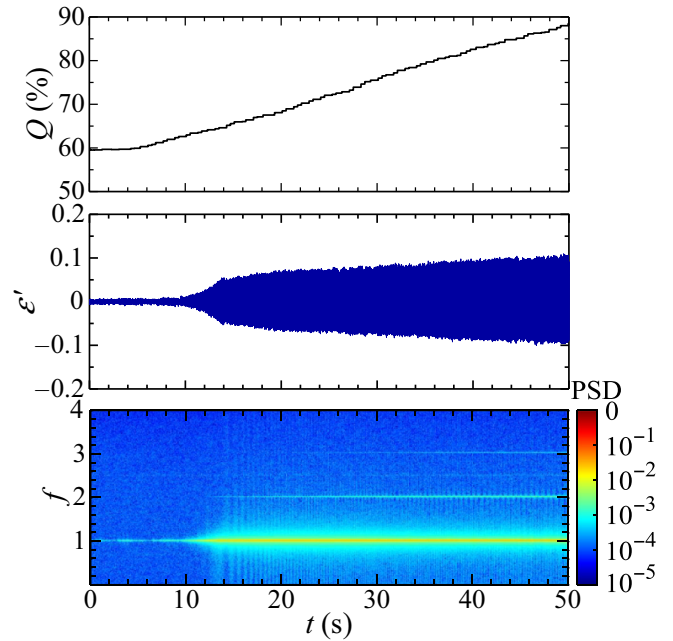


FIG. 2. Temporal evolution of strain fluctuations ϵ' at the 50th blade and the corresponding PSD with increasing mass flow rate of inlet air Q .

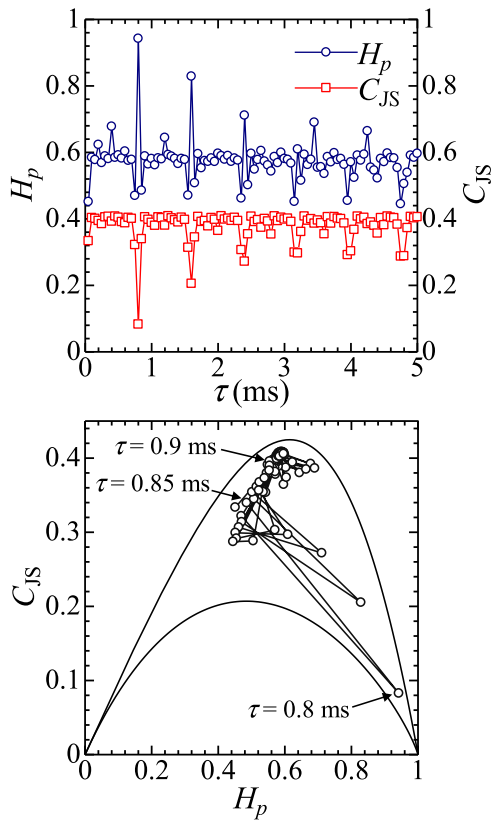


FIG. 3. Variations in permutation entropy H_p and Jensen–Shannon statistical complexity C_{JS} in terms of the embedding delay time τ , together with H_p – C_{JS} plane.

obtained by a stochastically driven van der Pol oscillator [36]. This indicates that the dynamical state of ϵ' represents noisy limit-cycle oscillations. Zhang and Small [24] have reported that multiple peaks appear (one dominant peak appears) in the degree distribution for deterministic nonperiodic intercycle dynamics (for periodic orbits with correlated noise, such as noisy periodic limit-cycle oscillations) and that the scale-free structure is (not) formed in the vertex-strength distribution. The degree distribution $p(k_i)$ and the vertex-strength distribution $p(S_i)$ in the cycle network are shown in Fig. 4. Note that the vertex strength S_i in the weighted cycle network is defined as $S_i (= \sum_j \rho_{ij})$. The multiple peaks and the scale-free structure are not observed in $p(k_i)$ and $p(S_i)$, respectively, indicating the formation of noisy periodic limit-cycle oscillations. These results show that the dynamical state of strain fluctuations during cascade flutter represents noisy limit-cycle oscillations. Multiple van der Pol oscillators with different dominant oscillation frequencies from each other start to oscillate at the same frequency through collective synchronization [37]. In our preliminary test, we observe the synchronization of oscillation frequencies for stochastically driven multiple van der Pol oscillators. On this basis, the dynamics of cascade flutter can be treated as a form of collective synchronization.

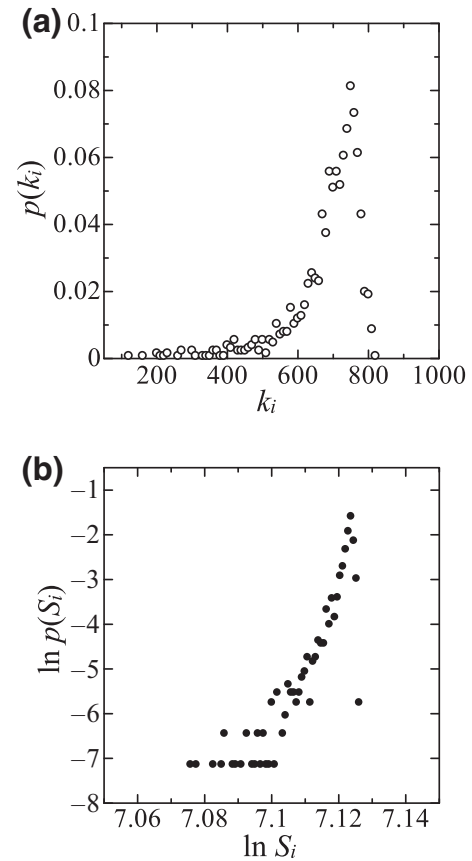


FIG. 4. (a) Degree distribution $p(k_i)$ in cycle network. (b) Vertex-strength distribution $p(S_i)$ in weighted cycle network during cascade flutter.

Figure 5 shows the variations in the connecting strength D_{mn} between the nodes and the network topology with increasing Q . Note that the connection of the nodes with $D_{mn} \leq 0.5$ is not displayed in the network topology. D_{mn} takes sufficiently low values at $t = 5.0$ s [Fig. 5(a)] and synchronized nodes are not formed. When $t = 11.0$ s [Fig. 5(b)], D_{mn} increases between the nodes from the 47th to the 51st blade. This shows that a locally synchronized state starts to appear at specific nodes as a signature of the initiation of flutter. The number of connecting nodes increases significantly at $t = 15.0$ s [Fig. 5(c)], and the node corresponding to the 50th blade forms the primary hub of the networks. In our preliminary test, we observe two important points: (i) the blades adjacent to the 50th blade start to oscillate at the same dominant frequency and (ii) the interblade phase angle at the 50th blade asymptotically takes an almost constant value. These findings indicate the onset of phase entrainment with the initiation of collective synchronization. The connection between the primary hub and the other nodes becomes much stronger with increasing Q . This means that the 50th blade is a significant driving source of cascade flutter. We clearly observe the emergence of a high D_{mn} between all the nodes

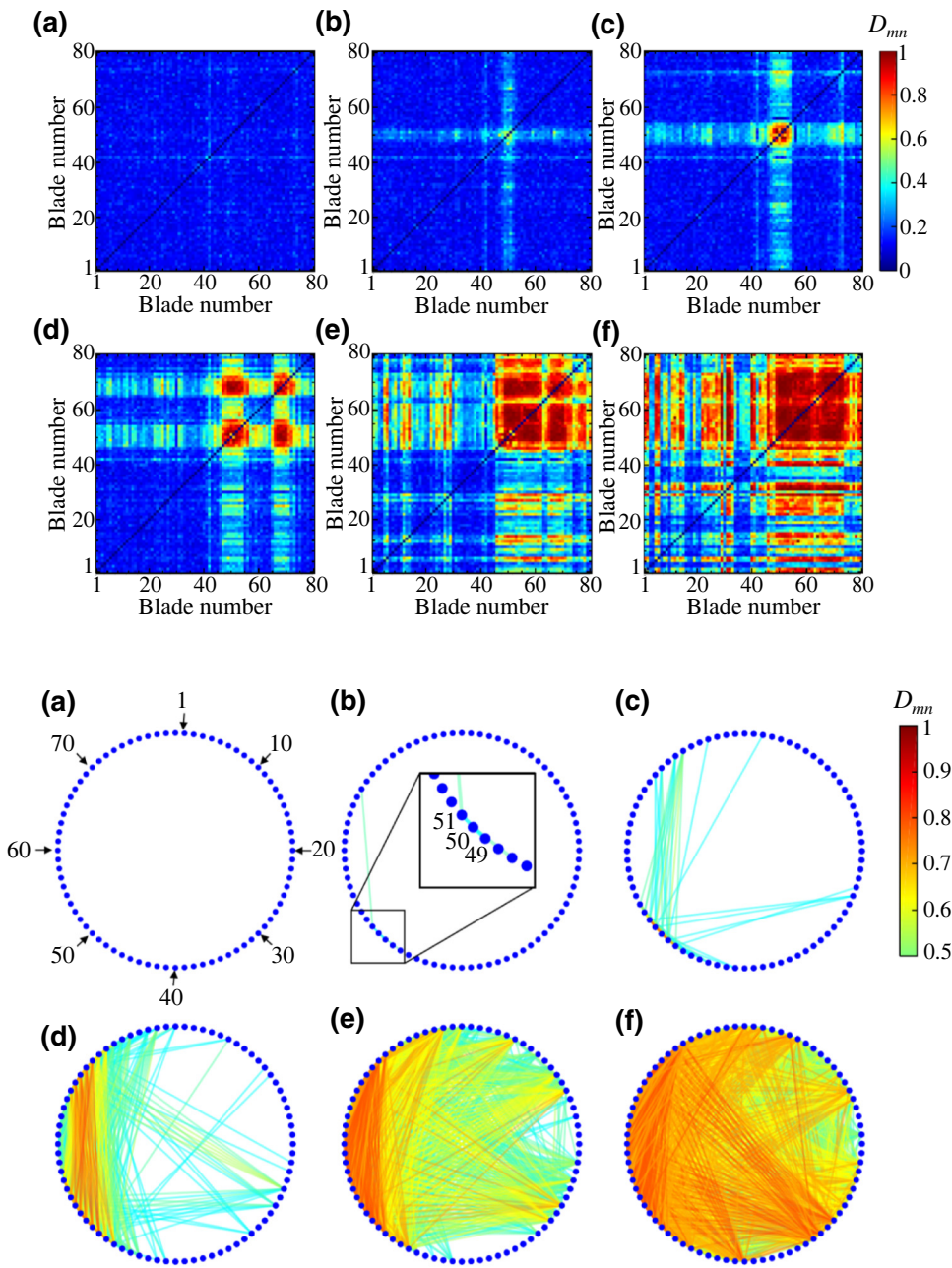


FIG. 5. Variations in connecting strength D_{mn} between nodes and network topology with increasing mass flow rate of inlet air Q : (a) $t = 5.0$ s; (b) $t = 11.0$ s; (c) $t = 15.0$ s; (d) $t = 22.0$ s; (e) $t = 30.0$ s; (f) $t = 45.0$ s.

at $t = 30.0$ s [Fig. 5(e)] as a result of collective synchronization between the vibrating blades. These results show that the network topology constructed from the determinism in CRPs allows us to extract the primary hub during a transition to collective synchronization. The temporal evolution of the node strength I with increasing Q is shown in Fig. 6. At around the 50th blade, I begins to significantly increase as t exceeds approximately 10 s. The 50th blade strongly interacts with the nearby blades as the primary hub of the networks, indicating the formation of a synchronous cluster. The cascade of the low-pressure turbine is designed to be axisymmetric, but it is accompanied by a slight change in the natural frequency of each blade.

This results in the formation of the synchronous cluster. The other blades take high values of I with increasing time, resulting in the emergence of collective synchronization between the vibrating blades. These results clearly show that the node strength is a useful network measure for capturing a precursor of cascade flutter.

Figure 7 shows the temporal evolution of the synchronization parameter r_s with increasing Q . When t exceeds approximately 10 s, r_s starts to increase owing to the formation of the synchronous cluster. We observe a further increase in r_s at $20 \text{ s} \leq t \leq 26 \text{ s}$, accompanied by the expansion of the synchronous-cluster region. This is attributed to the initiation of collective synchronization.

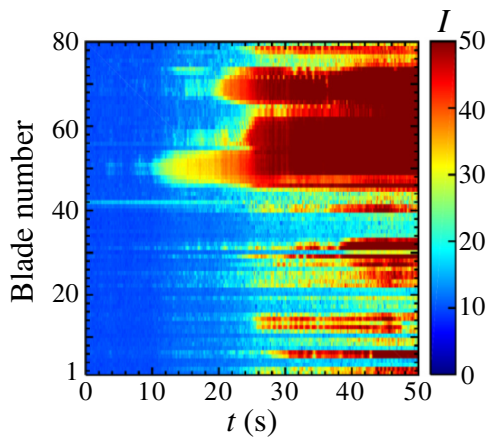


FIG. 6. Temporal evolution of node strength I in networks with increasing mass flow rate of inlet air Q .

An important point to emphasize here is that r_s can detect the significant transition to collective synchronization during cascade flutter. Our recent study [38] proposed a methodology combining symbolic dynamics, dynamical systems, and machine learning for detecting a precursor of cascade flutter. In this study, we mainly show the applicability of two important local and global measures as potential detectors of cascade flutter: the node strength and the synchronization parameter. The former is valid for specifying the dominant blades for the onset of cascade flutter. In contrast, the latter is more suitable for determining the threshold for the onset of cascade flutter because the synchronization parameter ranges from zero to unity. In addition to the recent methodology [38], the complex-network- and/or synchronization-based approach that we employ in this study would contribute to opening up the development of early detection of cascade flutter in turbofan jet engines.

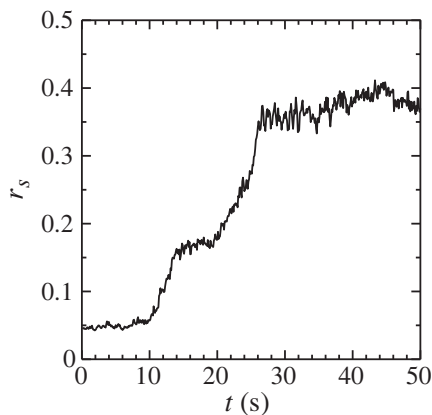


FIG. 7. Temporal evolution of synchronization parameter r_s with increasing mass flow rate of inlet air Q .

V. SUMMARY

We have conducted an experimental study on the early detection of cascade flutter in a model aircraft turbine using a methodology combining complex networks and synchronization, including the characterization of the dynamical state during cascade flutter. The multiscale complexity-entropy causality plane incorporating a time-dependent approach clearly shows that the dynamic behavior of strain fluctuations represents noisy limit-cycle oscillations during cascade flutter. The formation of noisy limit-cycle oscillations is reasonably identified by the cycle-network approach. The network topology constructed from the determinism in the CRP allows us to extract the primary hubs during a transition to collective synchronization. The node strength in the network topology and the synchronization parameter are valid for capturing a precursor of cascade flutter.

ACKNOWLEDGMENT

We thank Mr. Yuji Nomi (Tokyo University of Science) for the computation of the cycle network.

- [1] A. V. Srinivasan, Flutter and resonant vibration characteristics of engine blades, *J. Eng. Gas Turbines Power* **119**, 742 (1997).
- [2] G. M. L. Gladwell, *Solid Mechanics and Its Applications: A Modern Course in Aeroelasticity* (Kluwer Academic Publishers, Dordrecht, 2004), Vol. 216.
- [3] K. C. Hall, R. E. Kielb, and J. P. Thomas, *Unsteady Aerodynamics, Aeroacoustics and Aeroelasticity of Turbomachines* (Springer, 2006).
- [4] J. Venkatramani, V. Nair, R. I. Sujith, S. Gupta, and S. Sarkar, Precursors to flutter instability by an intermittency route: A model free approach, *J. Fluids Struct.* **61**, 376 (2016).
- [5] J. Venkatramani, V. Nair, R. I. Sujith, S. Gupta, and S. Sarkar, Multi-fractality in aeroelastic response as a precursor to flutter, *J. Sound Vibration* **386**, 390 (2017).
- [6] A. Pikovsky, M. Rosenblum, and J. Kurths, *Synchronization* (Cambridge University Press, New York, 2001).
- [7] Y. Kuramoto, *Chemical Oscillations, Waves, and Turbulence* (Dover Publications, New York, 2003).
- [8] S. Mondal, V. R. Unni, and R. I. Sujith, Onset of thermoacoustic instability in turbulent combustors: An emergence of synchronized periodicity through formation of chimera-like states, *J. Fluid Mech.* **811**, 659 (2017).
- [9] T. Hashimoto, H. Shibuya, H. Gotoda, Y. Ohmichi, and S. Matsuyama, Spatiotemporal dynamics and early detection of thermoacoustic combustion instability in a model rocket combustor, *Phys. Rev. E* **99**, 032208 (2019).
- [10] M. Small, *Applied Nonlinear Time Series Analysis: Applications in Physics, Physiology and Finance* (World Scientific, London, 2005).
- [11] S. Murayama, H. Kinugawa, I. T. Tokuda, and H. Gotoda, Characterization and detection of thermoacoustic

- combustion oscillations based on statistical complexity and complex-network theory, *Phys. Rev. E* **97**, 022223 (2018).
- [12] C. Aoki, H. Gotoda, S. Yoshida, and S. Tachibana, Dynamic behavior of intermittent combustion oscillations in a model rocket engine combustor, *J. Appl. Phys.* **127**, 224903 (2020).
- [13] H. Gotoda, H. Kinugawa, R. Tsujimoto, S. Domen, and Y. Okuno, Characterization of Combustion Dynamics, Detection and Prevention of an Unstable Combustion State Based on a Complex-Network Theory, *Phys. Rev. Appl.* **7**, 044027 (2017).
- [14] T. Kobayashi, S. Murayama, T. Hachijo, and H. Gotoda, Early Detection of Thermoacoustic Combustion Instability Using a Methodology Combining Complex Networks and Machine Learning, *Phys. Rev. Appl.* **11**, 064034 (2019).
- [15] T. Nishizawa, in *Proceedings of the International Gas Turbine Congress 2019 Tokyo, IGTC-2019-IL2* (2019).
- [16] H. Gotoda, H. Kobayashi, and K. Hayashi, Chaotic dynamics of a swirling flame front instability generated by a change in gravitational orientation, *Phys. Rev. E* **95**, 022201 (2017).
- [17] K. Takagi, H. Gotoda, I. T. Tokuda, and T. Miyano, Nonlinear dynamics of a buoyancy-induced turbulent fire, *Phys. Rev. E* **96**, 052223 (2017).
- [18] H. Kobayashi, H. Gotoda, S. Tachibana, and S. Yoshida, Detection of frequency-mode-shift during thermoacoustic combustion oscillations in a staged aircraft engine model combustor, *J. Appl. Phys.* **122**, 224904 (2017).
- [19] H. Kasuya, H. Gotoda, S. Yoshida, and S. Tachibana, Dynamic behavior of combustion instability in a cylindrical combustor with an off-center installed coaxial injector, *Chaos* **28**, 033111 (2018).
- [20] H. Kobayashi, H. Gotoda, and S. Tachibana, Nonlinear determinism in degenerated combustion instability in a gas-turbine model combustor, *Phys. A* **510**, 345 (2018).
- [21] K. Takagi and H. Gotoda, Effect of gravity on nonlinear dynamics of the flow velocity field in turbulent fire, *Phys. Rev. E* **98**, 032207 (2018).
- [22] T. Hachijo, S. Masuda, T. Kurosaka, and H. Gotoda, Early detection of thermoacoustic combustion oscillations using a methodology combining statistical complexity and machine learning, *Chaos* **29**, 103123 (2019).
- [23] W. Kobayashi, H. Gotoda, S. Kandani, Y. Ohmichi, and S. Matsuyama, Spatiotemporal dynamics of turbulent coaxial jet analyzed by symbolic information-theory quantifiers and complex-network approach, *Chaos* **29**, 123110 (2019).
- [24] J. Zhang and M. Small, Complex Network from Pseudoperiodic Time Series: Topology versus Dynamics, *Phys. Rev. Lett.* **96**, 238701 (2006).
- [25] N. Tani, M. Aotsuka, and J. Kazawa, Evaluation of torsion axis position on turbine blade flutter by direct measurement experiment: Rig design and numerical simulation, *Proc. ASME Turbo Expo 2016*, 57108 (2016).
- [26] JAXA ATF, <http://www.aero.jaxa.jp/facilities/aeroengine/facility02.html>.
- [27] J. Zhang, X. Luo, and M. Small, Detecting chaos in pseudoperiodic time series without embedding, *Phys. Rev. E* **73**, 016216 (2006).
- [28] J. P. Zbilut, A. Giuliani, and C. L. Webber, Detecting deterministic signals in exceptionally noisy environments using cross-recurrence quantification, *Phys. Lett. A* **246**, 122 (1998).
- [29] N. Marwan and J. Kurths, Nonlinear analysis of bivariate data with cross recurrence plots, *Phys. Lett. A* **302**, 299 (2002).
- [30] N. Marwan, M. C. Romano, M. Thiel, and J. Kurths, Recurrence plots for the analysis of complex systems, *Phys. Rep.* **438**, 237 (2007).
- [31] K. Takagi, H. Gotoda, T. Miyano, S. Murayama, and I. T. Tokuda, Synchronization of two coupled turbulent fires, *Chaos* **28**, 045116 (2018).
- [32] S. Murayama and H. Gotoda, Attenuation behavior of thermoacoustic combustion instability analyzed by a complex-network- and synchronization-based approach, *Phys. Rev. E* **99**, 052222 (2019).
- [33] J. Gómez-Gardeñes, Y. Moreno, and A. Arenas, Paths to Synchronization on Complex Networks, *Phys. Rev. Lett.* **98**, 034101 (2007).
- [34] R. Gutiérrez, A. Amann, S. Assenza, J. Gómez-Gardeñes, V. Latora, and S. Boccaletti, Emerging Meso- and Macroscales from Synchronization of Adaptive Networks, *Phys. Rev. Lett.* **107**, 234103 (2011).
- [35] S. Balusamy, L. K. B. Li, Z. Han, M. P. Juniper, and S. Hochgreb, Nonlinear dynamics of a self-excited thermoacoustic system subjected to acoustic forcing, *Proc. Combust. Inst.* **35**, 3229 (2015).
- [36] L. Zunino, M. C. Soriano, and O. A. Rosso, Distinguishing chaotic and stochastic dynamics from time series by using a multiscale symbolic approach, *Phys. Rev. E* **86**, 046210 (2012).
- [37] M. A. Barrón and M. Sen, Synchronization of four coupled van der Pol oscillators, *Nonlinear Dyn.* **56**, 357 (2009).
- [38] T. Hachijo, H. Gotoda, T. Nishizawa, and J. Kazawa, Experimental study on early detection of cascade flutter in turbo jet fans using combined methodology of symbolic dynamics, dynamical systems theory, and machine learning, *J. Appl. Phys.* **127**, 234901 (2020).